Porous Films

DOI: 10.1002/anie.201303594

Breath Figure Arrays: Unconventional Fabrications, Functionalizations, and Applications

*Hua Bai, Can Du, Aijuan Zhang, and Lei Li**

breath figure arrays · patterning · porous materials · self-assembly · thin films

***A** breath figure (BF) is the water droplet array that forms when moisture comes in contact with a cold substrate. This water droplet array has been widely utilized in the past two decades as a versatile soft template for the fabrication of polymeric porous films. Accordingly, the ordered pores on the polymer films formed with such a method are named a breath figure array (BFA). The BF templating technique is undergoing rapid development. Several unconventional BF processes have been established to prepare porous films with unique morphologies or primary materials, and various newly developed functionalization techniques have significantly improved the performance of polymeric films with BFA, leading to novel applications, including templates, biosensors, and separation membranes. These recent achievements will be described in this Minireview.*

1. Introduction

A breath figure (BF) is the fog that is formed upon breathing onto a cold surface, and it is named according to the mode of generation. The formation of BFs was first investigated by Aitken in 1893 and later, in 1911, by Lord Rayleigh.[1] Depending on the wetting properties of the surface, the condensed fluid can form either a uniform film, which appears dark (black BF), or an assembly of droplets, which scatters light and appears white (gray BF).[2] BF has long been used as a simple and effective method to detect oil contamination on glass surfaces, which is familiar to photographers using the wet-plate processing technique.[2a,3] Of course, there is no actual dependence on human breath for the formation of BFs, and all that is necessary is an oversaturated vapor contacting a cold substrate (solid or liquid) that provides a location for condensation. One example of such phenomenon is the formation of dew on the ground.

For a long time, BFs were considered to be an annoying natural phenomenon that needed to be fully suppressed. Only recently, in 1994, François et al. discovered the formation of an ordered polymeric porous film when a drop of star-shaped polystyrene (PS)/carbon disulfide (CS_2) solution was exposed to a flow of moist air.[4] The micrometer-sized pores exhibited a highly regular hexagonal arrangement after removing the upper layer of these films that is reminiscent of a honeycomb. Soon after, the relationship between the works of Lord Rayleigh and François was recognized: the honeycomb-structured porous films were the result of BFs on solution surface. Therefore, the ordered pores on the polymer film prepared with such a method were named the breath figure array (BFA). Compared with other templating and lithography techniques widely used to produce ordered pattern on polymer films, the BF process shows its advantage by using water droplets as the sacrificial templates, the removal of which is spontaneous. Furthermore, the condensed droplets are flexible with adjustable shape and size, which is beneficial for the control of the resultant patterns. Thus, this simple method opens new prospects in the field of porous films, with the technical advantages of low-cost and large area applicability.

Since the pioneer work by François, various types of polymers have been employed to fabricate BFA films with controlled pore size, ranging from hundreds of nanometers to hundreds of micrometers. Moreover, the corresponding mechanism of BF process and the influence of experimental conditions, such as polymer structure, solvent, substrate, temperature, and humidity level, on the BFA formation have been comprehensively summarized and discussed.[5] Here in this Minireview, we will mainly focus on the recent advances in the non-conventional preparations of BFAs promoted by newly developed techniques and materials. The applications

[*] Dr. H. Bai, C. Du, A. Zhang, Prof. L. Li
College of Materials, Xiamen University
Xiamen 361005 (P.R. China)
E-mail: lilei@xmu.edu.cn

of BFAs drive the rapid development of this field, thus we will also discuss the functionalization of BFAs, and especially emphasize the applications in lithography, separation, templating, biomaterial engineering, and optoelectronic devices.

2. Formation of BFAs

From a practical point of view, formation of BFAs is quite simple. The preparation process is shown in Figure 1 a. Typically, a solid substrate is placed into a humid environment, and a polymer solution is cast onto this substrate. After all of the solvent has evaporated, a polymer BFA film is left on the substrate. Depending on the way in which the humid

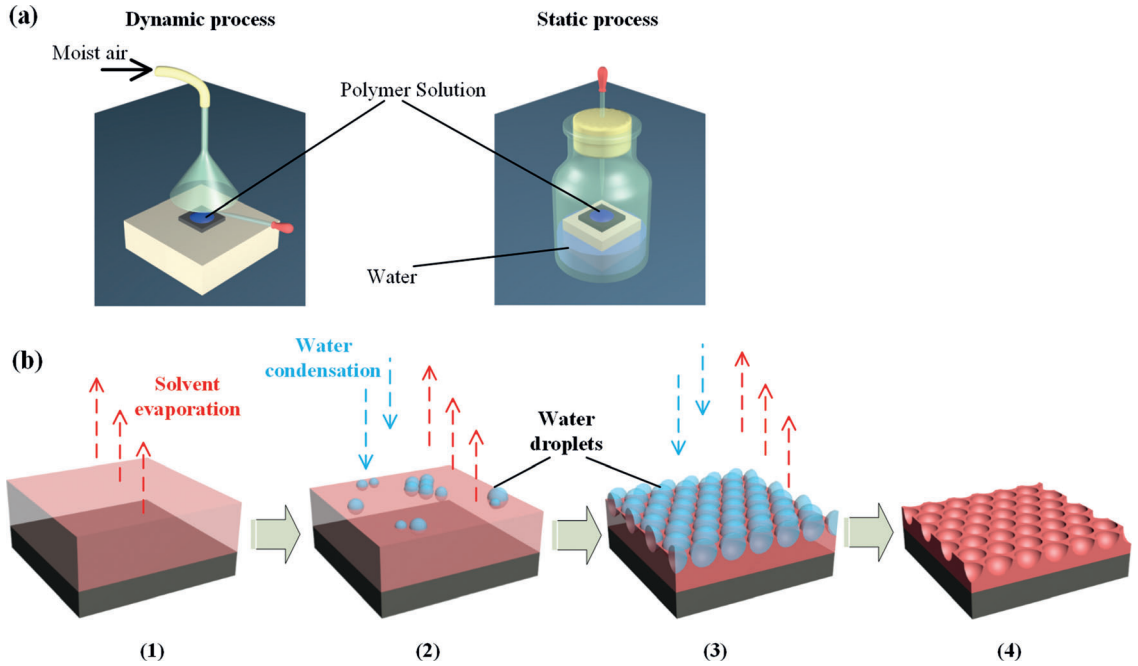

Figure 1. a) Representation of the preparation of BFAs by dynamic and static BF processes. b) Mechanism of BFA formation.

Hua Bai received his BS (2004) and PhD (2009) degree in Department of Chemistry at Tsinghua University under the supervision of Prof. Gaoquan Shi. From 2009 to 2011 he was a postdoctoral fellow in Department of Chemical Engineering at Tsinghua University. He is currently an associate professor in the College of Materials at Xiamen University. His research interests mainly focus on organic conjugated materials and graphene.

Can Du received his BE degree in the College of Materials at Xiamen University in 2011. He is currently pursuing his MS degree with Prof. Lei Li investigating porous materials.

Aijuan Zhang received her BE (2008) and MS degree (2011) from Xiamen University and Nankai University, respectively. She is currently a PhD candidate at the College of Materials, Xiamen University under the supervision of Prof. Lei Li. Her research interests are macromolecular self-assembly and porous materials.

Lei Li received his PhD in 2001 from China Textile University. After two-year postdoctoral experience at the Peking University, he joined the National Institute of Advanced Industrial Science and Technology (AIST) in Japan as a NEDO and JSPS research fellow. In 2007 he moved to the College of Materials, Xiamen University as a full professor. His research interests are living radical polymerization, functional polymers, and porous materials.

environment is established, the process can be divided into dynamic and static BF. In the dynamic BF process the moisture is supplied by a gas flow blowing over the substrate, while in the static BF process the substrate is sealed in a vessel saturated with water vapor. The formation mechanisms of BFAs have been discussed previously[6] and summarized in recent Reviews,[5] and the well-accepted principles involve the following processes (Figure 1b): 1) Evaporation of the organic solvent with low boiling point, leading to the cooling of the solution; 2) condensation of water vapor onto the cold solution surface, forming water droplets; 3) continuous condensation of water vapor, causing the growth and self-organization of the water droplets into ordered droplet array; and 4) complete evaporation of the organic solvent and then the water droplets, producing the BFAs. The formation of polymeric BFAs shows two distinct differences from that of mist on the cold window: the solution surface is soft, and thus the water droplets may float on or sink into the solution, resulting in a single or multiple layer of BFA; and the solute can strongly effect the formation and stability of the water droplets, because the adsorption or precipitation of solute at the droplet/solution interface is inevitable. Therefore, the seemingly simple process has complex thermodynamic and kinetic underpinnings which are not fully understood, resulting in many disputes and uncertainties over this formation mechanism.

The non-equilibrium nature of the BF process makes it sensitive to the experimental conditions. Furthermore, the BFA preparations reported so far were all performed on a home-made apparatus, which were different from each other in many structural details. As a result, the data from different groups are inconsistent, causing confusion in understanding the formation mechanism of BFAs. For example, Qiao et al. reported that the pore diameters decreased with increasing molecular weight,[7] whereas increasing molecular weight resulted in bigger pores in the system investigated by Stenzel et al.[8] The operation model also strongly influences the formation of BFAs. Usually, nonpolar linear polymers are not believed to be good candidates for BF technique, because they cannot form a solid polymer envelope to prevent the coalescence of water droplets, which is what star polymers do at the organic solvent–water interface.[8,9] As a result, in a dynamic BF process, linear PS resulted in regular films only under very specific conditions, and were very sensitive to the molecular weight and casting solvents.[10] However, in a static BF process, we have shown that linear PS without any polar end group could also form well-defined BFAs, tolerating a wide range of temperature, solution concentration, and molecular weight.[11] Therefore, to definitely clarify the formation mechanism of polymeric BFAs, systematic experiments and visible observations are needed, as demonstrated recently by François and Yunus.[6c,12] Also, some newly developed methods, such as BFA fabrication on nonplanar substrate, may help in the direct observation of the BFA evolution during solvent evaporation, as discussed in Section 3.

3. Unconventional Fabrication of BFAs

A conventional BF process, as described above, involves casting a polymer solution on a flat substrate in the humid environment, which yields polymer films with ordered pore array. However, in recent years, fabrication of BFAs with modified methods and particular materials other than polymers has been reported. The unconventional processes that are used to create BFAs not only offer BFAs with varieties of promising applications, but also shed light on the formation mechanism of BFAs.

3.1. Perforated BFAs

Polymer films with uniform perforation can act as separation membranes and masks. In most case studies, BFA films are formed on solid substrates, and there is always a bottom layer under the pore structures. By depositing a dilute solution of an amphiphilic polymer on water surface, a self-standing honeycomb mesh was formed. This "on-water spreading" method was first developed by Shimomura et al.[13] Calculations by Wan et al. indicate that the interfacial tension of soft substrate is essential for the formation of perforated BFAs.[14] With the evaporation of the casting solvent, the polymer solution film becomes thinner than the diameter of water droplets, and consequently a meniscus forms under the water droplet, where the water droplets and substrate liquid are separated by a thin polymer film (Figure 2, inset). The pressure difference, induced by the surface

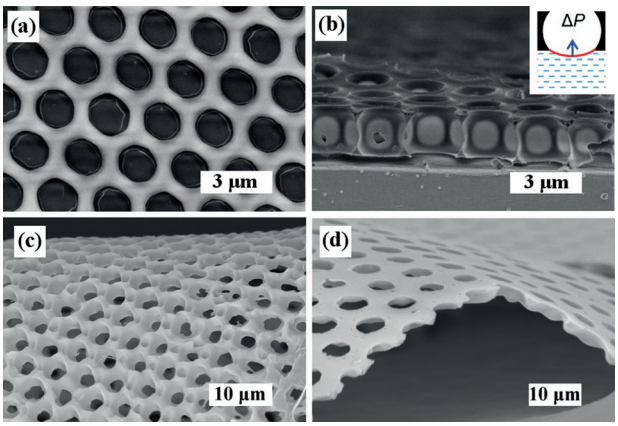

Figure 2. Scanning electron microscope (SEM) images of honeycomb-structured membranes with through-pores, prepared by a),b) polystyrene-*b*-poly-(*N*,*N*-dimethylaminoethyl methacrylate) at an air–ice interface[14] and c),d) SIS on glass substrate:[16] a),c) top views, b),d) cross-sectional views. Inset of b) illustrates the formation mechanism of through-pores. Reprinted with permission from Refs. [14, 16]. Copyright 2012 and 2013 American Chemical Society.

tension of the substrate liquid across the meniscus during evaporation of water droplets, should exceed the critical pressure at which the thin polymer film ruptures, generating perforated pores (Figure 2a,b). Therefore, through-pores can form on the surface of glycerol and formic acid with high interfacial tension, but not on those with low interfacial

tension, such as acetic acid, tetraethyl orthosilicate, ethyl acetate, ethanol, isopropanol, and methanol. Furthermore, perforated monolayer films of dodecanethiol-stabilized gold nanoparticles were fabricated by Hao et al. using the same technique.[15] Recently, our group developed a versatile method to prepare perforated BFA films on solid substrate (Figure 2c,d).[16] The key step is that the excess solution underneath the floating droplets array is sucked out rapidly. With the descending solution surface, the floating droplets contacted with and were squeezed by the substrate, resulting in a rupture of the thin interfacial polymer layer. As a result, the water droplets adhered to the substrate and through-pore structures appeared after complete evaporation of the solvent and water.

3.2. BFAs in Non-aqueous Vapors

The influence of the vapor atmosphere on the formation and morphology of BFA seldom attracts attention. Nearly all BFAs are fabricated under water vapor, and organic vapors are not believed to be suitable for BFA formation because of their miscibility with the casting solvents (Typically CS_2 or chloroform ($CHCl_3$)). The first investigation on BFA formation with block copolymer, polystyrene-*block*-polydimethylsiloxane (PS-*b*-PDMS), under methanol and ethanol vapors was reported by our group.[17] Ordered BFAs were found under both alcohol vapors (Figure 3). For the BFA formation under water atmospheres, the spherical pores were buried inside the films, thus the opening sizes were smaller than the maximal diameters of the pores (Figure 3a). However, cylindrical pores with a U-shape section separated by thin walls were found in the BFAs prepared under methanol vapor (Figure 3c). When the atmosphere was changed to ethanol vapor, ellipsoidal pores were observed (Figure 3e). The shape of the pores is determined by the resultant force of surface tension, buoyancy, and gravity of the template droplets, and liquid droplets with small surface tension, such as methanol droplets, will be elongated by buoyancy and gravity, yielding anamorphic pores. Besides, the pore size in these BFAs is also different, in inverse proportion to the enthalpy of vaporization of the atmosphere solvents. Surely, the influence of polymer chemical nature on the BFA formation cannot be excluded in the non-aqueous vapor BF process, as both linear and amphiphilic polymers never formed ordered structures with the same process. However, we still believe that changing the atmosphere will become a new means to adjust the morphology and pore size of BFAs.

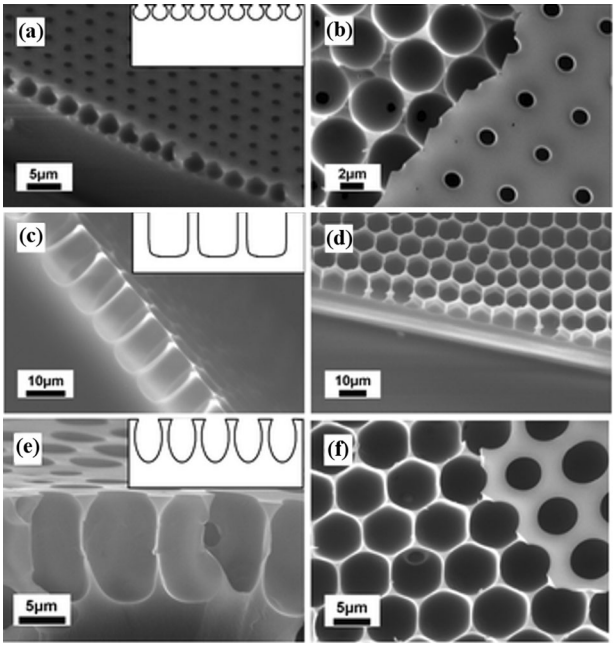

Figure 3. SEM images showing the shapes of pores in the polymer films prepared under different vapor atmospheres. Cross-section views of films produced in water, methanol and ethanol atmospheres are shown in (a), (c), and (e), respectively, and the contour lines of the section of the pores are shown in the insets. The corresponding top views of honeycomb arrays in the three films after peeling off the top layer are shown in the right column in (b), (d), and (f).[17] Reproduced by permission of The Royal Society of Chemistry.

3.3. BFAs on Non-planar Substrate

Patterning a non-planar substrate is still challenging for lithography techniques. Recent studies showed that BF technique could provide a simple method to fabricate micropatterns on non-planar substrates.[18] The first systematical work was completed by Qiao et al. utilizing a series of core cross-linked star polymers (CSPs) based on PDMS on the surface of transmission electron microscope (TEM) grids, as well as other non-planar surfaces (Figure 4a,b).[18b–e] Only the CSPs with T_g below 48 °C can form homogeneous BFAs on non-planar substrates, while the other CSPs with higher T_g only produce cracked film without ordered pores. This polymer allows the film to conform to the surface without the underlying topography lost, which is possibly due to relaxation of the very low T_g films. Recently, they further demonstrated that the elasticity in CSPs is a more important factor, compared with T_g, in determining the occurrence of cracking during the BFA formation on non-planar surfaces.[18d]

However, we demonstrated that neither the molecular topography nor the T_g of polymers was the key factor in forming uniform BFAs on non-planar substrates during a static BF process.[18a] Either linear polymers PS or block copolymer, polystyrene-*block*-poly(acrylic acid) (PS-*b*-PAA) or commercially available triblock copolymer polystyrene-*block*-polyisoprene-*block*-polystyrene (SIS), perfectly replicated non-planar substrates with a static BF process.[18a,f] To explain how a brittle polymer film can contour the curved structures, a hypothesis involving polymer plasticization by solvent during BF process has been proposed. The dramatically plasticized polymer layer has a fluid-like character, and is able to be contoured on the non-planar substrate without cracking.

Particularly, the observation of BFAs on non-planar substrates with vertical walls is helpful for the mechanism investigation (Figure 4c–f).[18a,f] Different from flat substrate,

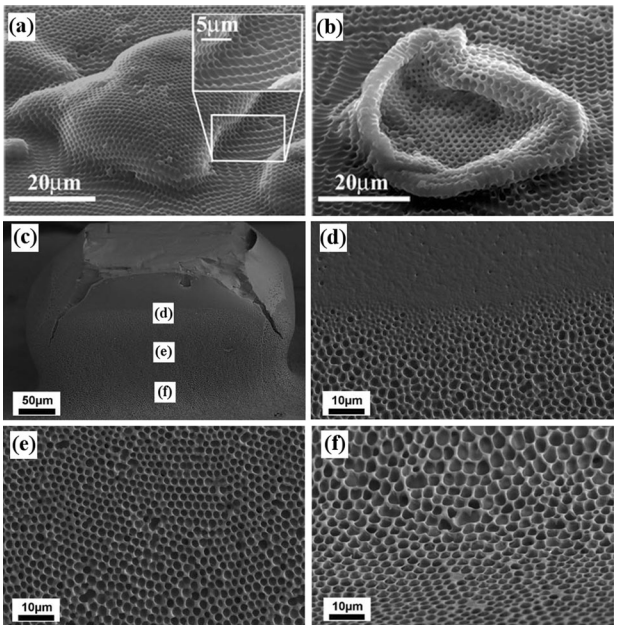

Figure 4. a) SEM images of a sugar crystal, coated with star PDMS honeycomb film, and b) the structure after dissolution of the sugar crystal.[18c] c)–f) SEM images of PS-*b*-PDMS porous film on sugar crystal with static BF process. c) A panorama of the crystal covered with porous PS-*b*-PDMS film. d)–f) Magnified images of the corresponding areas in c).[17] Reproduced from Refs. [17, 18c], with permission from The Royal Society of Chemistry.

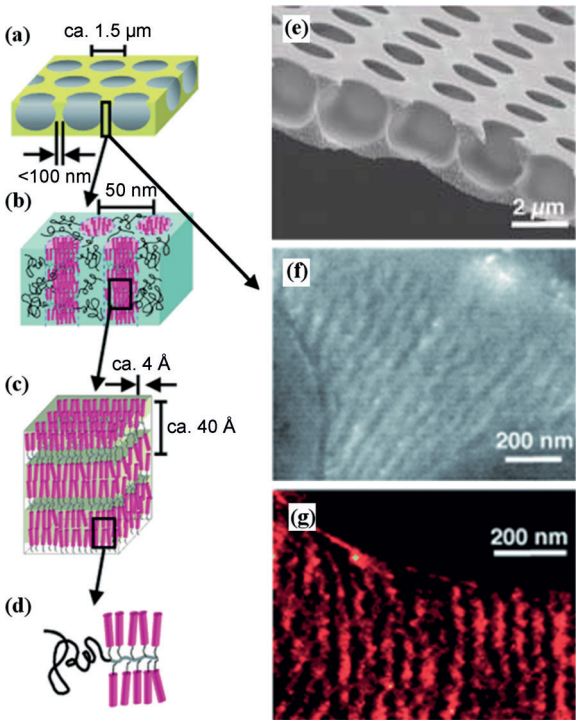

Figure 5. a)–d) Representation of the self-organized hierarchical structure of the semi-rod–coil block copolymer: a) microsized porous structure, b) nanosized phase-separated structure of PS and oligothiophene-modified side chains (POTI), c) oligothiophene with molecularly orientated smectic A liquid-crystalline structure in POTI nanophase-separated domains, d) molecular structure of the semi-rod–coil block copolymer. e) SEM image of the self-organized microporous structure, f) TEM image of perpendicular cross-section view of the microporous film, and g) the corresponding sulfur-distribution image.[19d] Reprinted with permission from Ref. [19d].

a capillary force between the descending solution surface and the vertical wall is induced owing to the decrease in the amount of solution as the solvent evaporates. Consequently, the BFAs floating on the solution surface will be pulled towards the vertical wall and cover it. With the decrease of the polymer solution level, the BFAs at different stages can be fixed onto the wall at different heights after the solvent and water dry up. In our experiment, increasing in pore size and degree of order was observed as the solution descended from the top of the vertical wall (Figure 4c–f), indicating the evolution of the BFAs in the whole BF process.

3.4. BFAs with Hierarchical Order

For a wide range of advanced technological devices incorporating organic materials, it is desirable, advantageous, and often necessary that the hierarchical structures of these materials are precisely controlled in multiple scales. With self-organization, the hexagonal BFA patterns make up one level of the hierarchical structures. Another level can be provided by either micro-phase-separated diblock copolymers[19] or nanoparticles[20] on smaller scale, or the external templates on larger scale.[18a,21] Hayakawa and Horiuchi synthesized a semi-rod–coil block copolymer containing mesogenic oligothiophene on the side chains.[19d] A self-organized three tiers of hierarchical structures within a polymer film from angstroms to micrometers with the combination of a liquid crystal phase, phase-separated nanodomain structures formed by block copolymers and ordered honeycomb structure forming in BF process is achieved by molecular design and a simple process (Figure 5). Other hierarchically ordered BFAs were prepared with the assistance of templates. When the above-mentioned TEM grids serve as non-planar substrates for BFA formation, they provide ordered mesh with a width of tens to hundreds of micrometers (Figure 6a). Therefore hierarchically ordered polymer films were prepared on these substrates, as reported by Qiao et al.[21a,b] Alternatively, two other approaches were also reported: 1) Post-photo-cross-linking of BFAs in the presence of a photomask and dissolving the uncross-linked part, also producing hierarchically ordered structure (Figure 6b);[21d] and 2) placing a grid template on the surface of the evaporating solution, leading to formation of BFAs only in the mesh space of the grid (Figure 6c,d).[21e]

3.5. BFAs Based on Non-polymeric Materials

Although BFAs are usually prepared from polymer solutions, the formation of BFAs actually does not require the present of polymer in solution. Any solute that is able to stabilize the water droplets and form a continuous film can be used to replace polymer, producing non-polymeric BFAs. By now a number of non-polymeric materials have been used for

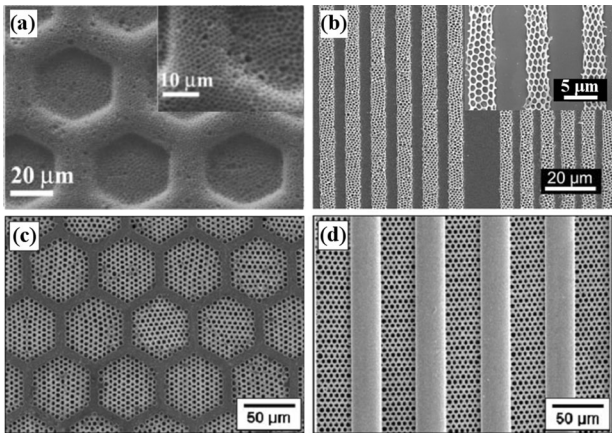

Figure 6. SEM images of a) a honeycomb structured film formed on the surface of 600 mesh hexagonal TEM grid;[21b] b) the patterned honeycomb lines achieved by the lithography;[21d] c,d) hierarchical structure fabricated by placing c) a hexagonal grating or d) a parallel grating on the surface of the evaporating solution.[21e] Insets show higher magnification of a) and b), respectively. Reprinted with permission from Refs. [21b,d,e].

the fabrication of BFAs. Generally, these materials fall into three categories: nanoparticles (especially metal/metal chalcogens),[22] carbon materials,[23] and small organic molecules.[21d,24]

Nanoparticles are the most attractive because of their unique photonic, electronic, and catalytic properties. Notably, amphiphilicity is crucial for the formation of metal nanoparticle BFAs. The nanoparticles must be dispersible in organic solvent, and also have suitable hydrophilicity to accumulate on the water/oil interface to stabilize the water droplets. Thus, nanoparticles are usually encapsulated with surfactants or hydrophobic alkyl groups. Gold[22a,c–e] SiO_2, TiO_2, and CdS[22f] BFAs have been successfully prepared following these strategies. For example, gold BFAs were fabricated with dioctadecyldimethylammonium chloride modified gold nanoparticles,[22a] and CdS BFAs were prepared with a thiol ($C_nH_{2n+1}SH$) modified CdS nanoparticle dispersion in chloroform. The length of the alkyl chain of surfactants was reported to be an important factor which determined the morphology of the BFA film. For thiol-modified CdS particles, the thiols with $n = 10$–12 are optimum; only CdS modified with such thiols can produce ordered BFA film, because they have suitable solubility and hydrophilicity.[22f] Besides, if the nanoparticles are thermostable, the surfactants in nanoparticle BFA films can be removed by calcination without damaging the structure of the BFAs, producing pure inorganic BFAs.[22f] Carbon materials, including carbon nanotubes (CNTs) and graphene, recently were employed to fabricate BFAs.[23] Similar to metal nanoparticles, CNTs and graphene need covalent or non-covalent modification to make them dispersible in organic solvents. For example, polymer-grafted graphene oxide (GO) platelets were dispersed in benzene and fabricated into BFA film.[23a] In another work, GO was decorated non-covalently by dimethyldioctadecylammonium (DODA) with a phase-transfer method, and became oil-dispersible.[23b] Free-standing BFA film was obtained with such decorated GO by casting with $CHCl_3$. These GO BFAs could be further converted into graphene BFAs by pyrolysis[23a] or hydrazine reduction[23b] (Figure 7a). Nakashima et al. reported the fabrication of

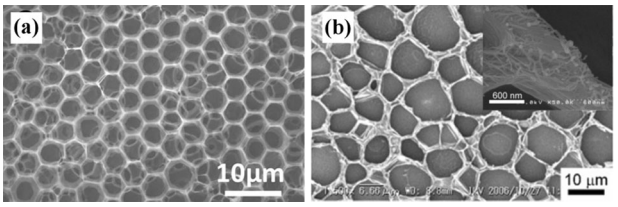

Figure 7. SEM images of a) reduced graphene oxide (RGO) films prepared by hydrazine reduction of GO/DODA complex BFAs,[23b] and b) CNT BFAs cast from a chloroform solution after ion exchange.[23d] Inset shows higher magnification (scale bar 600 nm) of (b). Reprinted with permission from Refs. [23b,d].

CNT BFAs on glass and flexible PET film by using a shortened-single-walled CNTs-lipid conjugate and sequent removing lipid by an ion-exchange method (Figure 7b).[23c,d] These carbon materials are conductive and biocompatible, and thus the BFAs based on them may have potential applications in electrochemistry and tissue engineering. Small organics are usually inefficient in stabilizing water droplets and thus seldom used as the primary materials for BFAs. Recently, it was found that the supramolecular aggregates of several small molecules, whose structures were shown in Scheme 1, could effectively stabilize water droplets and form BFAs.[21d,24] For example, BFA films were prepared by Ajayaghosh et al. using aggregates of small amphiphilic molecules (Scheme 1e).[24c] These molecules were able to form supramolecular aggregates by hydrogen bonds and π–π interactions, yielding a fibrillar network and stabilizing water droplets during the BF process.

4. Chemical Reactions and Functionalizations in BFAs

The control of surface properties and chemical functions is one of the essential goals for the construction of porous materials. Although the BF process is compatible with various functional materials, in many cases chemical reactions are still needed to improve the performance of the materials. During the BF process, polar functional groups on the polymer chains are oriented in the pores of BFAs by the water droplet templates;[12,25] also in a polymer/nanoparticle mixture, the added nanoparticles selectively gather and enrich on the walls of the pores owing to the Pickering-emulsion effect.[26] These spontaneous chemical heterogeneity benefits further surface modification which endows the film with new functionalization. Furthermore, light, heat, or vulcanization can induce the cross-link reactions in the polymeric films, significantly changing the thermal and chemical stability as well as the surface wettability of the BFA films. The recent development of chemical functionalization of BFAs is summarized in this section.

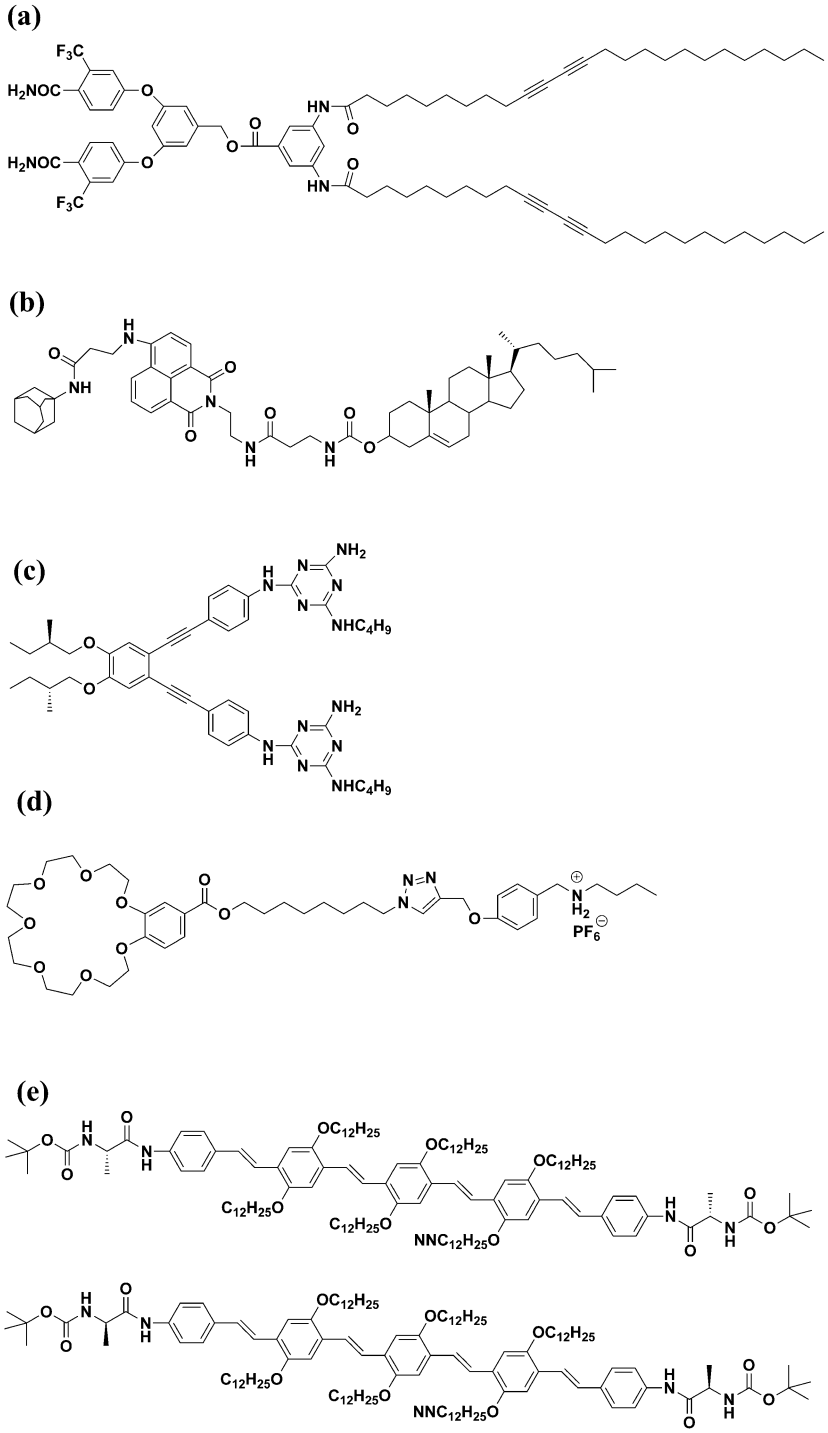

Scheme 1. Molecular structures of small organics used as blocking matreials for the fabrication of BFAs.[21d,24]

4.1. Surface Modification

Surface modification is necessary for BFA films with specific applications.[25b,d,27] For example, a fluorinated and rough surface showing excellent superhydrophobic properties was created by CF_4 etching.[27a] Surface graft polymerization can be achieved by controlled/living radical polymerization. As mentioned above, hydrophilic segments, which act as the grafting site, always gather on the inner surface of the pores; the hydrophobic ones aggregate inside the film and on the top layer of the film. Therefore it is possible to selectively modify the inner surface of the pores. Wan et al. applied surface-initiated atom-transfer radical polymerization (ATRP) to functionalize the inner surface of the pores in BFA for the preparation of carbohydrate microarrays, which was suitable for specific recognition of lectin.[25d] Stenzel et al. sequently grafted thermo-responsive monomers *N*-isopropyl acrylamide (NIPAAm) and *N*-acryloyl glucosamine (AGA) onto

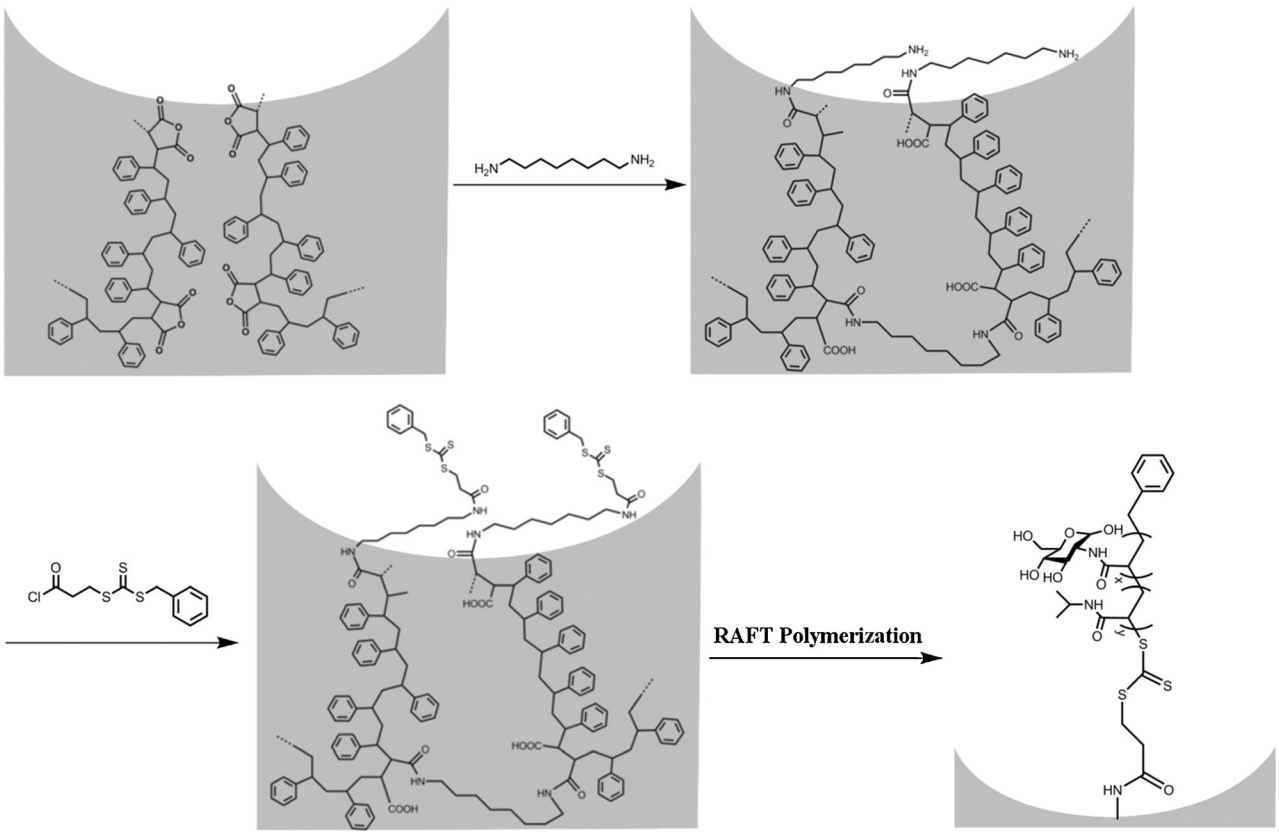

Scheme 2. Preparation of cross-linked poly(styrene-*co*-maleic anhydride) BFA films and subsequent grafting of thermo-responsive glycopolymers PNIPAAm-*ran*-PAGA by RAFT polymerization inside the pores.[27c]

BFA films by reversible addition-fragmention chain transfer (RAFT) (Scheme 2).[27b,c] As a result, the films displayed switchable hydrophilic/hydrophobic characteristics and turned into a thermodependent switcher for selective recognition of biomolecules. Click reaction was also used to graft side chains onto cellulosic BFAs.[28]

4.2. Cross-linking

Cross-linking is an efficient method of improving the thermal and chemical stability of polymeric BFAs for their practical application in a harsh environment. By molecular design, cross-linkable groups can be easily introduced into the polymer backbone or side-chains. Heat,[29] ultraviolet (UV) light,[11,18b,30] or chemicals[18f,31] are able to initiate the cross-linking reactions.

Usually, thermal treatment will inevitably cause the polymeric microstructure to completely or partially collapse before the temperature-sensitive groups totally cross-link. To prevent this, a two-step thermal treatment was developed by Galeotti and co-workers.[29a] First, a liquid PDMS precursor was poured into the BFAs and solidified at a temperature lower than the T_g of the polymer matrix. With further increase of the temperature, the thermal cross-linkage in polymer matrix was initiated and the PDMS elastomer that covered the surface and filled the pores of the film worked as a memory mask for maintaining the microstructure of BFAs. After cooling, the cross-linked film became solvent-resistant while the surface structure was perfectly preserved.

The photochemical cross-linking is a non-destructive technique to cross-link polymer thin films. Double-bond-containing polymers are ideal candidates for photochemical cross-linkage. Shimomura et al. prepared bas-relief patterns by selectively UV irradiating honeycomb films containing poly(1,2-butadiene) through photomasking.[30d] After heat treatment, the uncross-linked film was melted and the remaining pattern showed a very distinct edge, with a 4% resolution error (Figure 8). UV irradiation not only improves the film robustness but also changes the film surface wettability from hydrophobicity to hydrophilicity. Therefore, the UV irradiated polystyrene-*b*-polybutadiene-*b*-polystyrene (SBS) BFA surface with a pore size close to 3 μm is a better matrix for cell adhesion and spread than a commercially available culture dish.[30c]

Linear PS and PS-containing block copolymers can also be photochemically cross-linked, although the mechanism, shown in Scheme 3, is still in dispute.[32] In this photoreaction, the radicals are generated at α position of the backbone and migrate along the polymer chain. When two radicals are close to each other, the cross-linking may occur. The cross-linked PS BFA films are resistant to a wide range of organic solvents and temperature up to 250 °C. More importantly, the UV cross-linked PS-*b*-PAA has a char yield of 40% at 450 °C, and

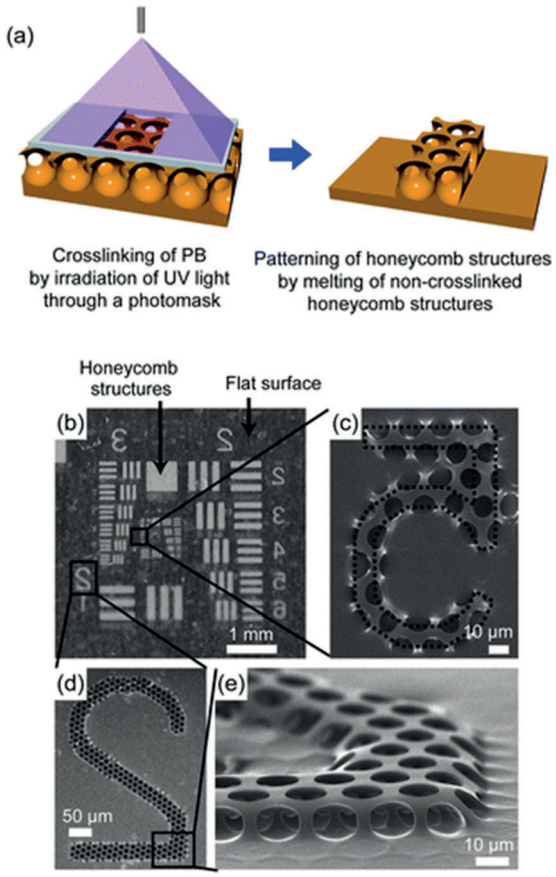

Figure 8. a) Illustration of the fabrication of patterned honeycomb film. b) Photograph and c)–e) SEM images of the patterned honeycomb film[30d] (dashed lines show the mask pattern size). Reproduced from Ref. [30d] with permission from The Royal Society of Chemistry.

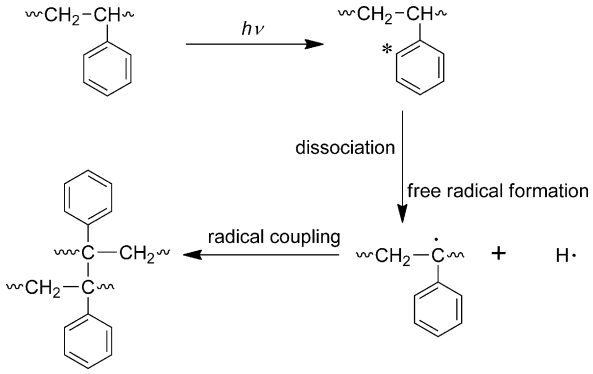

Scheme 3. Possible cross-linking mechanism of PS under deep UV irradiation.

thus can work as a structure-directing agent to grow CNT and zinc oxide (ZnO) nanorod arrays, which will be discussed in Section 5.

It was proposed by Stenzel et al. that chemical cross-linking should lead to increased stability of honeycomb films.[31b] Karthaus et al. prepared mesoporous honeycomb films from poly(styrene-*co*-maleic anhydride).[31a] Cross-linkage was achieved by immersion in an ethanol solution of an α,ω-alkyldiamine. The cross-linked honeycomb structure was stable up to 350 °C, an increase of more than 150 °C as compared to the uncross-linked films. Our group used S_2Cl_2 vapor to vulcanize SIS BFA film, and significantly increased its mechanical strength and chemical stabilities.[31c] The sulfidity is related to the vulcanization time.

4.3. Hybrid BFAs

Hybridization of organic materials with inorganic constituents may combine the merits of both components, and many inorganic compounds can endow the hybrid materials with additional reactivity. In the system of hybrid BFAs, inorganic compounds are introduced for new functionalities. To prepare hybrid BFAs, the inorganic nanocomponent is mixed with a polymer solution and the blend solution is cast following a standard BF process. It is worth noting that nanoparticles may self-assemble at the polymer-solution/water-droplet interface and benefit the stabilization of water droplets (Pickering-emulsion effect).[20a,26,33] The total free-energy change for the process of moving a particle from a polymer solution onto the solution/water interface is determined by:

$$\Delta G = -\pi r^2 \gamma_{O/W}(1+\cos\theta_{O/W})^2 \quad (1)$$

where r is the particles radius, $\gamma_{O/W}$ the water–oil interfacial tension, and $\theta_{O/W}$ the contact angle at the water–oil interface.[34] Therefore, as long as the particle is amphiphilic ($0 < \theta_{O/W} < 180$), the free energy change ΔG is always negative and the accumulation of particles at the interface is spontaneous (however, if $|\Delta G|$ is as small as kT, detachment of the particles from the interface becomes easy, driven by Brownian motion). Russell et al. employed fluorescence confocal microscopy, TEM, and SEM to confirm the preferential segregation of the ligand-stabilized CdSe nanoparticles to the polymer solution/water interface (Figure 9 a–e).[26] Also from Equation (1) it can be deduced that $|\Delta G|$ falls rapidly with particle size, as confirmed by Ji et al., who demonstrated that the larger nanoparticles presented a much better interfacial stabilizing performance and thus enhanced the regularity of BFA (Figure 9 f).[20a] Other nanomaterials, such as CNTs,[35] hydrophilic nanoclays,[36] alkyl stabilized metals,[33a] surfactant-encapsulated polyoxometalates,[37] dye-loaded zeolite L crystals,[33c] and even unmodified metal[33b] have been reported to stabilize water and to form hybrid BFAs. Furthermore, hybrid BFAs can also be prepared by directly attaching inorganic materials to polymers through non-covalent interactions.[38]

5. BFA Applications

There have been great efforts devoted to exploit applications of BFAs. The major characteristics of BFAs are the ordered pore array on a soft film, with adjustable size and shape. Thus, BFA films are widely used as templates to guide the formation of other materials. Besides, BF technique is

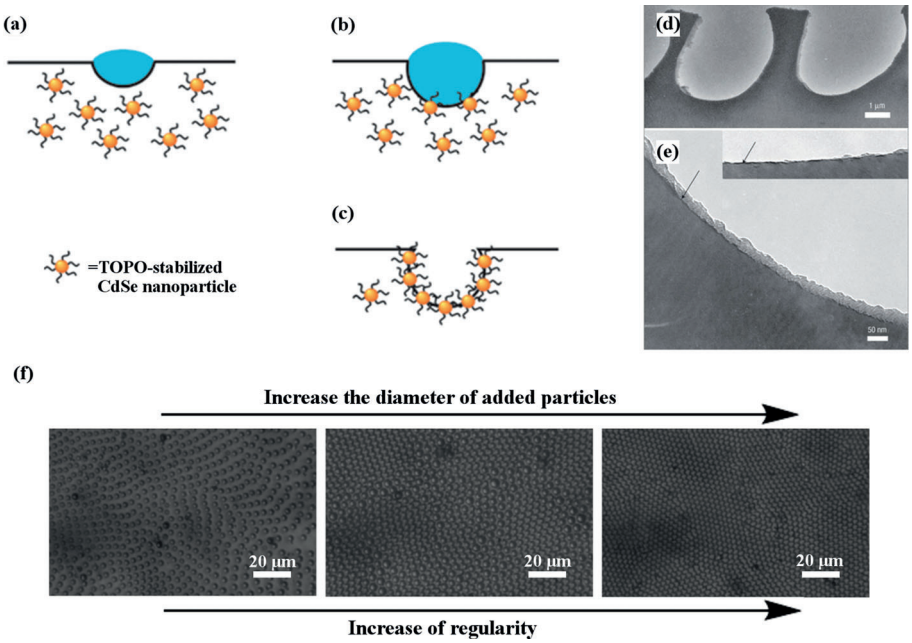

Figure 9. a)–c) Illustration of the formation process of hybrid BFAs. The particles segregate to the solution–water interface during drying of the solution. d) Overview of micrometer-sized holes. e) Magnification of the polymer–air interface, where the CdSe nanoparticles can be seen as a thin black layer (arrowed). The inset shows another spot at the polymer–air interface inside one of the holes.[26] Reproduced with permission from Ref. [26]. Copyright 2004, rights managed by Nature Publishing Group. f) Optical microscope images of PS BFA films prepared from solutions containing silica particles with diameters of 100 nm, 200 nm, and 1000 nm (from left to right), respectively.[20a] Reprinted with permission from Ref. [20a]. Copyright 2008 American Chemical Society.

compatible with many kinds of polymers and materials with various functions. Other applications of BFAs mainly focus on how to utilize the pattern or the pores of BFAs and combine the functions of materials with their unique morphology. In this section, several important applications of BFAs will be summarized.

5.1. Breath Figure Templating Applications

One of the most important uses of BFAs is templating applications. It allows us to convert polymeric BFAs into honeycomb structure based on other materials, which cannot be directly utilized in BF process. Compared with other widely used templates, such as colloidal crystals and block copolymer patterns, the BF process is versatile and low-cost, because of its pore size adjustability and easy preparation. BFAs have been combined with different techniques, such as in situ pyrolysis, hydrolyzing,[39] vapor deposition,[40] electroless plating,[41] regioselective self-assembly,[42] and crystal growth,[43] to create various novel materials. In the following section several representative works are discussed.

A polymeric BFA matrix can act as the structure-directing agent to guide the formation of inorganic micro-patterns if an inorganic precursor is embedded.[44] Usually the cross-linking of a polymeric BFA matrix is needed before pyrolysis, to prevent the melting and collapsing of the honeycomb structure, although sometimes the inorganic precursor itself can also stabilize the microstructure.[44a] During the pyrolysis process, the organic polymer matrix is decomposed whereas the inorganic precursor is simultaneously converted into inorganic micropatterns with the guidance of the cross-linked polymer matrix. For example, our group has demonstrated that by using 3-amino-propyltrimethoxysilane (APETS), zinc acetylacetonate ($Zn(acct)_2$), and ferrocene as precursors, silica, ZnO, and ferric oxide (Fe_2O_3) honeycomb patterns can be prepared by prolyzing corresponding cross-linked PS-*b*-PAA/precursor composite BFAs (Figure 10a–c).[45] Moreover, the obtained honeycomb inorganic microstructure is able to play the role of either catalyst or nuclear site, to further direct the growth of other materials.[45,46] ZnO nanorod honeycomb microstructures (Figure 10d) were grown with a hydrothermal method on the above-mentioned ZnO honeycomb pattern, and aligned honeycomb CNTs patterns were also successfully grown by chemical vapor deposition (CVD) (Figure 10e), with the honeycomb Fe_2O_3 pattern as the catalyst (Figure 10c).[45,46] Interestingly, if PS-*b*-PAA/ferrocene BFA film was used directly as a catalyst in the CVD process, CNT array would grow from the pores in BFA film (Figure 10f) owing to enrichment of ferrocene in the water/polymer solution interface.[46] In some special cases, polymers themselves are precursors of inorganic materials, thus they can produce inorganic honeycombs without additional reactants.[47] Two examples of such polymers are hyperbranched poly(phenylene vinylene) (PPV)[47b] and PS-*b*-PDMS;[47c] BFAs based on these polymers can be converted by pyrolysis into honeycomb carbon and silica, respectively.

Replica molding is another widely used technique to produce microstructured film in which BFAs are commonly employed as templates. This technique is usually applied to prepared polymeric microstructures. During replica molding, either a polymer solution of a prepolymer is poured onto BFA

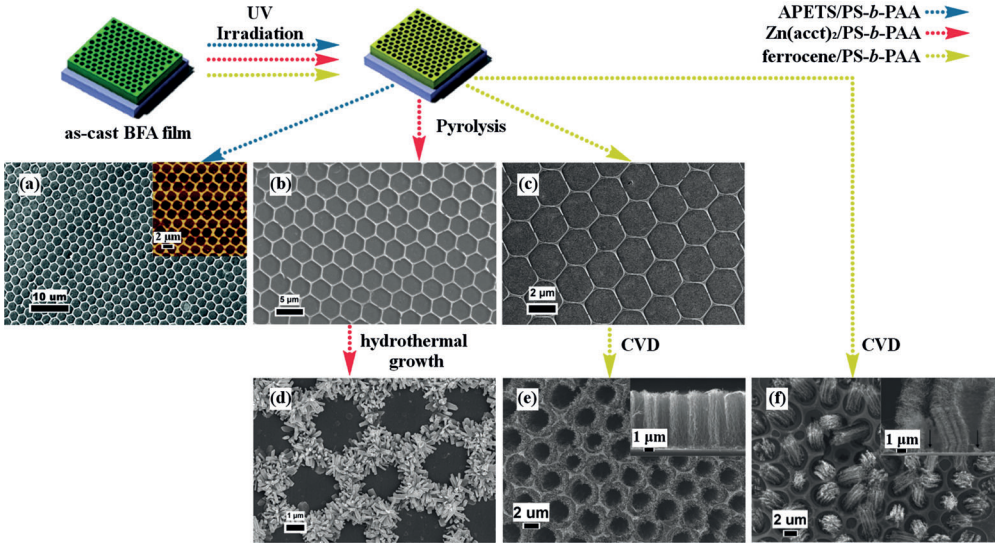

Figure 10. Pictures of the fabrication process of a) silica, b) ZnO, and c) Fe_2O_3 honeycomb patterns by pyrolysis of cross-linked PS-*b*-PAA/precursor composite BFAs, and d) ZnO nanorods and e) aligned CNTs grown from (b) and (c) by a hydrothermal process and CVD, respectively. f) A SEM image of CNT bundles synthesized from as-prepared PS-*b*-PAA/ferrocene BFAs by CVD.[45,46] Insets show AFM images of the silica honeycomb pattern and the cross-sectional SEM images of aligned CNTs patterns, respectively. Reprinted with permission from Refs. [45] and [46]. Copyright 2009 and 2010 American Chemical Society.

film and is allowed to fill the micropore arrays. After drying or curing, a polymer film with microstructure can be released from the BFA film. As BFAs are the close-packed array of micropores, the molds of BFAs are the arrays of microspheres or micropillars. PDMS is widely used in BFA replica molding owing to its low surface energy. Combined with soft lithography, various patterns can be printed using PDMS replicas. For example, PDMS micropillar array was prepared by Galeotti et al. molded from PS BFAs, and further used as a stamp to prepare quantum dot patterns by soft lithography technique.[48] Other materials, such as polypyrrole, silk, and poly(methyl methacrylate) (PMMA), were also used for replica molding of BFAs.[49] It should be noted that the shape and arrangement of pores in BFAs can be changed by stretching the BFA films, thus the anomalous structure is obtained by molding from such deformed BFA film.[50]

Recently, a new method, called breath figure lithography (BFL), has been established as an economical and facile way to produce micropatterns on substrates over centimeter length scales. To perform BFL, a honeycomb structured mask is first prepared using BFA, and then the pattern is transferred onto substrates through etching.[51] Typically, the top layer of BFA films, a thin membrane with ordered perforated pores, can be peeled off and used as the mask for etching process.[51a,d] A patterned metal layer fabricated by sputter-coating on BFA film is also a good mask.[51b,c] The patterned metal layers can be prepared following two routes, giving different masks: 1) Sputter-coating vertically on the BFAs, peeling off the top layer, and dissolving the polymer matrix, which leaves ordered metal circular patterns on the substrate;[51c] and 2) sputter-coating slantwise and dissolving the polymer matrix, which leaves a metal honeycomb pattern on the substrate.[51b] Using the above two masks, different micropatterns are transferred onto silicon substrates.

5.2. Applications in Biosensors and Biomaterials

In recent years, a host of biocompatible and biodegradable polymers, including poly (ε-caprolactone), poly (L-lactide), polyalkylcyanoacrylate, glycopolymer, DNA, and their copolymers, have been used as building blocks for BFAs for bio-scaffolding.[52] These biocompatible BFAs always show enhanced performance of cell attachment, spreading, and proliferation compared with the unpatterned polymer films.[50b,52d,f,53] The pore size and shape of BFA have considerable influence on the cell behavior: the enhanced effect of cell adhesion, spreading, and proliferation are more prominent with the decrease of pore size,[50b,54] and there seems to exist a threshold pore size for cell adhesion, which is dependent on the chemical properties of the polymer;[55] when the films are stretched, cells proliferate along the direction of the long axis of the micropores.[50] Furthermore, the chemical properties of the film and the surface also play important roles in cell behavior.[56] It has been shown that increasing hydrophilicity is beneficial for enhancing the adhesion of the cells on honeycomb-structured porous films.[27b,52c,57] Protein BFAs were also produced after selectively grafting protein recognization moieties on the surface of the pores.[58] As mentioned above, hydrophilic sequences gather on the inner surface of pore and serve as the grafting site, and thus almost all the proteins are selectively immobilized into the pores, forming hexagonally arranged microwells of proteins.

Biomaterial BFAs are also used for other biomedical applications besides cell culture. John and co-workers studied the release characteristics of poly(lactic-*co*-glycolic acid) (PLGA) honeycomb films, which showed a higher release rate compared to the unpatterned films.[52b] Wan et al. prepared glucose-sensing films based on phenylboronic acid

(PBA) pendants, which segregated at the pore wall of BFAs induced by the template water droplets.[59] Alizarin Red S (ARS) was attached to PBA pendants as the fluorescent probe, and high glucose sensitivity of the functionalized BFAs was demonstrated by quartz crystal microbalance results (Figure 11). They also hybridized enzymes into BFAs to prepare honeycomb patterned porous biocatalytic films with high activity.[60] For applications in cell culture and other biomedical applications, a common requirement is an antibacterial property. Recently, Chen et al. demonstrated the antibacterial activity of BFAs consisting of graphene and dimethyldioctadecylammonium.[23b]

5.3. Optical and Optoelectronic Applications

Periodic microstructures usually have interesting optical properties. In fact, the appearance of color caused by light diffraction can be utilized to judge whether ordered BFAs exists on a polymer film. Other functions of BFAs have also been exploited in optical and optoelectronic devices. Briefly, two different types of applications were developed: the ordered structures of BFAs were used to fabricate micro-optical device arrays, and the rough surface of BFAs was employed to reduce the light reflection and increase the light harvest. These applications are discussed below.

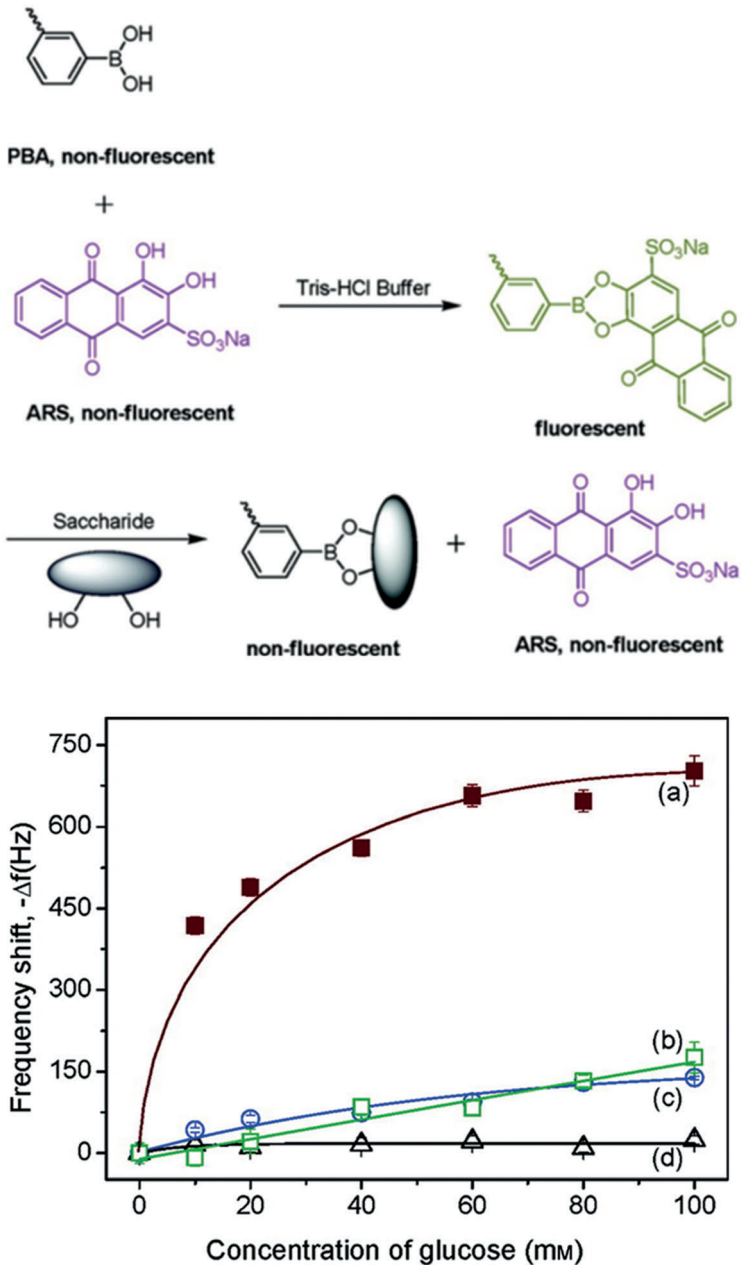

Figure 11. Illustration of the interaction among ARS, saccharide, and PBA. Quartz crystal microbalance (QCM) results of different films exposed to glucose solution. Honeycomb-patterned porous films of PS_{141}-*b*-P($AA_{0.5}$-*co*-$AAPBA_{13.5}$) a) after being prewetted with ethanol and b) without being prewetted; c) dense films. d) Honeycomb-patterned porous films of PS_{141}-*b*-PAA_{14} after being prewetted with ethanol.[59] Reprinted with permission from Ref. [59]. Copyright 2011 American Chemical Society.

The microlens array (MLA) is of special importance in many practical applications, such as optical elecommunication, solid state lighting, and displays. The micropores in BFA are spherical, becoming a perfect template for the fabrication of MLA. The principal means of fabricating MLA from BFA is molding. For example, Shimomura et al. prepared two PDMS MLAs with a spherical and hemispherical microlens by molding from as-prepared BFA film and BFA film with the top layer peeled off, respectively (Figure 12).[61] These MLAs were able to project miniaturized images. A similar PDMS MLA was reported to be able to increase the light intensity of organic light-emitting diodes (OLED) at 30–60° after it was patched outside the device, owing to the refraction of microlens.[62] Chari and colleagues modified the above process and produced anamorphic MLAs using UV-curable urethane methacrylate with higher mechanical strength and light refracting index.[63] The anamorphic ellipsoidal microlens array was molded from stretched BFA film, on which the micropores were elongated. This anamorphic MLA is able to modulate the angular distribution of luminance.

Another microdevice array produced from BFA is the OLED array, which has a potential application in high-resolution displays. Two methods have been developed to fabricate OLED arrays with BFA as template, and in both methods a MLA-like PDMS film molded from BFA was first prepared as an elastic stamp. With this PDMS stamp and electroluminescent polymer solution as ink, Bolognesi et al. printed a dot-array light-emitting layer for OLED.[64] The luminescent spots in the array had diameters of about 1 μm, and were expected to provide a high display resolution of 640 000 pixel/mm^2. Bradley et al. tried a different way of producing a patterned hole transport layer (HTL) using a MLA-like PDMS stamp.[65] The continuous active layer and other layers were then deposited onto the patterned HTL. They found that the OLED microarray showed a higher efficiency than ordinary devices with continuous structure; enhanced light extraction by microstructure was believed to be a major cause of the high efficiency.

In many optical devices, the decrease of light reflection or enhancement of light harvest is very important. BFA coatings have found their applications in these devices. Usually, light reflects at the air/solid and solid/solid interface, and a common way to reduce the reflection is to destruct the original interface and construct a new interface. Depending on the wavelength of the incident light, the mechanism of reflection reduction by BFA coating may be different. Kim and Park constructed cellulose acetate butyrate (CAB) film with multilayered BFA by a modified BF process, and found that this BFA coating with the proper thickness can reduce the near-IR (NIR) reflectivity of glass from over 4% to less than 1%.[66] They found that the pore sizes on different BFA layers are unequal, creating a gradually increased refractive index from the top to the glass substrate. This gradually increased refractive index makes the destructive interference occur in

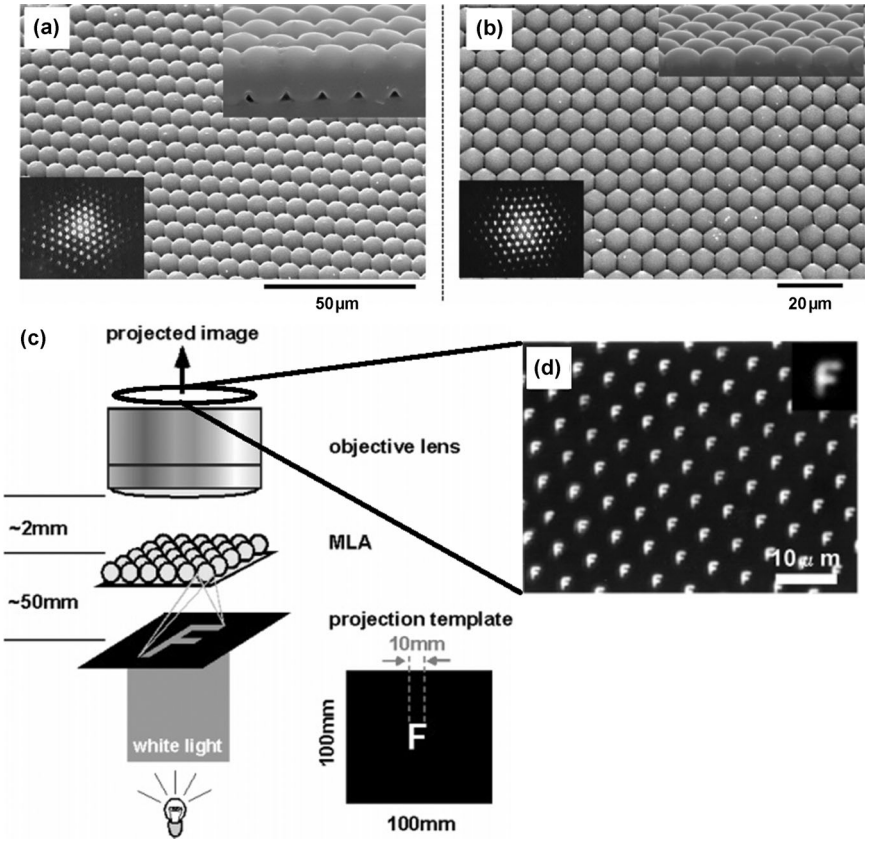

Figure 12. SEM images of a) a spherical MLA and b) a hemispherical MLA. Laser diffraction patterns and cross-sectional images are inserted in left and upper right corners of SEM images, respectively. c) Experimental setup of the projection experiment. d) Optical micrograph of projected images through the hemispherical MLA.[61] Reprinted with permission from Ref. [61]. Copyright 2005 American Chemical Society.

broad band of NIR. However, for visible and UV light, the cases are different because usually the pattern in BFA are larger than the wavelength of these light. Comparing with the smooth surface, the rough surface with BFA can reflect light iteratively insides its microholes, thus enhances the light harvest by multiple adsorption.[23b,38d,67] For example, under that same condition, photodetectors with honeycomb structure showed a larger photocurrent than its planar counterpart because of the antireflection effect of BFA.[67]

5.4. Separation Applications

Size-based separation is an important application area of porous polymeric membranes, including microfiltration for clarification and sterile filtration, and ultrafiltration for protein concentration. The BFAs with through-pore as mentioned above are good candidates for microsieves. Cong et al. prepared perforated brominated poly(phenylene oxide) BFA films with pore sizes ranging from 4.5 to 1.0 μm by adjusting the solution concentration. A maximum water flux of 25 $m^3 h^{-1} m^{-2}$ was achieved under a feed pressure of 0.13 MPa.[68] Wan et al. prepared polystyrene-*block*-poly(*N*,*N*-dimethylaminoethyl methacrylate) (PS-*b*-PDMAEMA) BFA film with perforated pores on soft substrate with a pore size of 3 μm.[14] The film shows high-resolution separation performance of polystyrene particles with a bimodal size distribution peaking at 2.0 and 5.0 μm. Unfortunately, the strength of the linear copolymer is weak, and the filter membrane has to be supported by stainless steel woven wire mesh. Recently, our group demonstrated that vulcanized SIS BFA films with perforated pores showed good mechanical properties and excellent chemical and thermal stability.[16] The pores on the microsieve forming in the BF process are highly ordered and tunable, ranging from 1 to 7 μm. Owing to the cross-linked chemical structure, this kind of microsieve is resistant to a variety of organic solvents, acidic, or basic and hot water. The vulcanized SIS microsieve successfully separates microparticles in hot water and tetrahydrofuran (THF). These characteristics make the vulcanized SIS membrane an ideal microsieve, which has potential application in industry.

6. Conclusion and Prospects

Inspired by a common natural phenomenon, the BF process together with many other modification and functionalization techniques has become a novel and robust way to create micro- and submicrostructures. Recent advances in the fabrication of unconventional BFAs, including perforated BFAs, BFAs in non-aqueous vapor, BFAs in non-planar substrates, and BFAs based on non-polymeric materials, have strongly pushed this field forward. Also, a growing number of applications of BFAs, such as templating, biosensors and biomaterials, optoelectronic and separation, have been exploited, demonstrating the eminent usefulness of BFAs. Although the preparation methodology and practical applications of BFAs have progressed tremendously, a well-established formation mechanism is still being sought. It is difficult to precisely predict the pore formation and morphology of this system, but meanwhile, a non-equilibrium state can be advantageous owing to the possibility of constructing structures that are not available in an equilibrium state by simply adjusting the processing conditions. A larger empirical database will allow the construction of a more complete set of rules to seek surprisingly new findings.

In our opinion, the future challenge will include the following three points:

1) How to prepare large-scale, defect-free BFAs. Defects, including non-uniform pore sizes, polydomain structures and disordered arrangement of pores, are usually found on BFA films, especially on those with large area. Reducing defects is essential for the practical application of BFAs. Several theories have been proposed to explain the formation of defects on BFA films. A possible reason for a wide pore size distribution is that the water droplets cannot be effectively stabilized to avoid coalescing during the early BF process. The domain boundaries may stem from the insufficient rearrangement of the water droplets because of the increasing solution viscosity during solvent evaporation.[69] Missing holes in BFAs, causing defects, may result from water droplets sinking into the polymer solution and finally being covered by the polymer layer.[70] New strategies must be put forward to avoid these imperfection.
2) How to unambiguously elucidate the mechanism of BFA formation. As discussed above, the design of new BFAs strongly relies on experience, but elucidation of the mechanism will definitely promote the development of BF method.
3) How to further exploit the new functions and applications of BFAs. To achieve this goal, new materials available in BF process must be exploited, while novel post-functionalization methods are also desirable. Recently, BF process also have aroused the interest of industry; a patent by Fuji Film Company demonstrated their interest in equipment which could produce BFA films continuously on a commercial scale.[71]

Therefore, with the combined efforts from polymer, chemistry, physics, and materials science, we believe that BF technique will undergo a rapid development and there will be breakthroughs in both theoretical and practical aspects of the BF technique in the near future.

L. Li gratefully acknowledges the National Natural Science Foundation of China (No. 21174116, 51035002 and 20974089) and the Key Laboratory for Ultrafine Materials of Ministry of Education.

Received: April 27, 2013
Published online: October 2, 2013

[1] a) L. Rayleigh, *Nature* **1912**, *90*, 436 – 438; b) L. Rayleigh, *Nature* **1911**, *86*, 416 – 417.
[2] a) T. J. Baker, *Philos. Mag.* **1922**, *44*, 752 – 765; b) J. Aitken, *Proc. R. Soc. Edinburgh* **1893**, *20*, 94.
[3] R. Merigoux, *Rev. Opt.* **1937**, *9*, 281 – 296.

[4] G. Widawski, M. Rawiso, B. François, *Nature* **1994**, *369*, 387 – 389.
[5] a) U. H. F. Bunz, *Adv. Mater.* **2006**, *18*, 973 – 989; b) M. H. Stenzel, *Aust. J. Chem.* **2002**, *55*, 239 – 243; c) H. Ma, J. Hao, *Chem. Soc. Rev.* **2011**, *40*, 5457 – 5471; d) P. Escalé, L. Rubatat, L. Billon, M. Save, *Eur. Polym. J.* **2012**, *48*, 1001 – 1025; e) M. Hernández-Guerrero, M. H. Stenzel, *Polym. Chem.* **2012**, *3*, 563 – 577.
[6] a) A. Steyer, P. Guenoun, D. Beysens, C. Knobler, *Phys. Rev. B* **1990**, *42*, 1086 – 1089; b) C. T. Kuo, Y. S. Lin, T. K. Liu, H. C. Liu, W. C. Hung, I. M. Jiang, M. S. Tsai, C. C. Hsu, C. Y. Wu, *Opt. Express* **2010**, *18*, 18464 – 18470; c) O. Pitois, B. François, *Colloid Polym. Sci.* **1999**, *277*, 574 – 578; d) B. Zhao, J. Zhang, X. Wang, C. Li, *J. Mater. Chem.* **2006**, *16*, 509 – 513; e) H. Ma, L. Kong, X. Guo, J. Hao, *RSC Adv.* **2011**, *1*, 1187 – 1189.
[7] L. A. Connal, P. A. Gurr, G. G. Qiao, D. H. Solomon, *J. Mater. Chem.* **2005**, *15*, 1286 – 1292.
[8] M. H. Stenzel-Rosenbaum, T. P. Davis, A. G. Fane, V. Chen, *Angew. Chem.* **2001**, *113*, 3536 – 3540; *Angew. Chem. Int. Ed.* **2001**, *40*, 3428 – 3432.
[9] a) B. François, Y. Ederlé, C. Mathis, *Synth. Met.* **1999**, *103*, 2362 – 2363; b) K. H. Wong, M. Hernández-Guerrero, A. M. Granville, T. P. Davis, C. Barner-Kowollik, M. H. Stenzel, *J. Porous Mater.* **2006**, *13*, 213 – 223.
[10] a) J. Peng, Y. Han, Y. Yang, B. Li, *Polymer* **2004**, *45*, 447 – 452; b) L. Cui, J. Peng, Y. Ding, X. Li, Y. Han, *Polymer* **2005**, *46*, 5334 – 5340.
[11] L. Li, Y. Zhong, J. Li, C. Chen, A. Zhang, J. Xu, Z. Ma, *J. Mater. Chem.* **2009**, *19*, 7222 – 7227.
[12] S. Yunus, A. Delcorte, C. Poleunis, P. Bertrand, A. Bolognesi, C. Botta, *Adv. Funct. Mater.* **2007**, *17*, 1079 – 1084.
[13] T. Nishikawa, R. Ookura, J. Nishida, K. Arai, J. Hayashi, N. Kurono, T. Sawadaishi, M. Hara, M. Shimomura, *Langmuir* **2002**, *18*, 5734 – 5740.
[14] L. S. Wan, J. W. Li, B. B. Ke, Z. K. Xu, *J. Am. Chem. Soc.* **2012**, *134*, 95 – 98.
[15] H. Ma, J. Cui, A. Song, J. Hao, *Chem. Commun.* **2011**, *47*, 1154 – 1156.
[16] C. Du, A. J. Zhang, H. Bai, L. Li, *ACS Macro Lett.* **2013**, *2*, 27 – 30.
[17] J. Y. Ding, A. J. Zhang, H. Bai, L. Li, J. Li, Z. Ma, *Soft Matter* **2013**, *9*, 506 – 514.
[18] a) J. Ding, J. Gong, H. Bai, L. Li, Y. Zhong, Z. Ma, V. Svrcek, *J. Colloid Interface Sci.* **2012**, *380*, 99 – 104; b) L. A. Connal, R. Vestberg, C. J. Hawker, G. G. Qiao, *Adv. Funct. Mater.* **2008**, *18*, 3315 – 3322; c) L. A. Connal, G. G. Qiao, *Soft Matter* **2007**, *3*, 837 – 839; d) Z. Zhang, T. C. Hughes, P. A. Gurr, A. Blencowe, X. Hao, G. G. Qiao, *Adv. Mater.* **2012**, *24*, 4327 – 4330; e) L. A. Connal, R. Vestberg, P. A. Gurr, C. J. Hawker, G. G. Qiao, *Langmuir* **2008**, *24*, 556 – 562; f) L. Li, Y. Zhong, J. Gong, J. Li, C. Chen, B. Zeng, Z. Ma, *Soft Matter* **2011**, *7*, 546 – 552.
[19] a) A. Muñoz-Bonilla, E. Ibarboure, E. Papon, J. Rodriguez-Hernandez, *Langmuir* **2009**, *25*, 6493 – 6499; b) K. H. Wong, T. P. Davis, C. Barner-Kowollik, M. H. Stenzel, *Polymer* **2007**, *48*, 4950 – 4965; c) P. Escalé, M. Save, A. Lapp, L. Rubatat, L. Billon, *Soft Matter* **2010**, *6*, 3202 – 3210; d) T. Hayakawa, S. Horiuchi, *Angew. Chem.* **2003**, *115*, 2387 – 2391; *Angew. Chem. Int. Ed.* **2003**, *42*, 2285 – 2289.
[20] a) W. Sun, J. Ji, J. Shen, *Langmuir* **2008**, *24*, 11338 – 11341; b) S. I. Matsushita, N. Kurono, T. Sawadaishi, M. Shimomura, *Synth. Met.* **2004**, *147*, 237 – 240.
[21] a) Z. Zhang, X. J. Hao, P. A. Gurr, A. Blencowe, T. C. Hughes, G. G. Qiao, *Aust. J. Chem.* **2012**, *65*, 1186 – 1190; b) L. A. Connal, G. G. Qiao, *Adv. Mater.* **2006**, *18*, 3024 – 3028; c) T. Ohzono, T. Nishikawa, M. Shimomura, *J. Mater. Sci.* **2004**, *39*, 2243 – 2247; d) J. H. Kim, M. Seo, S. Y. Kim, *Adv. Mater.* **2009**, *21*, 4130 – 4133; e) J. S. Park, S. H. Lee, T. H. Han, S. O. Kim, *Adv. Funct. Mater.* **2007**, *17*, 2315 – 2320.
[22] a) H. Ma, J. Hao, *Chem. Eur. J.* **2010**, *16*, 655 – 660; b) D. Fan, X. Jia, P. Tang, J. Hao, T. Liu, *Angew. Chem.* **2007**, *119*, 3406 – 3409; *Angew. Chem. Int. Ed.* **2007**, *46*, 3342 – 3345; c) P. S. Shah, M. B. Sigman, C. A. Stowell, K. T. Lim, K. P. Johnston, B. A. Korgel, *Adv. Mater.* **2003**, *15*, 971 – 974; d) J. Li, J. Peng, W. Huang, Y. Wu, J. Fu, Y. Cong, L. Xue, Y. Han, *Langmuir* **2005**, *21*, 2017 – 2021; e) X. M. Cai, K. W. Cheng, C. C. Oey, A. B. Djurišić, W. K. Chan, M. H. Xie, P. C. Chui, *Thin Solid Films* **2005**, *491*, 66 – 70; f) Y. Sakatani, C. Boissière, D. Grosso, L. Nicole, G. J. A. A. Soler-Illia, C. Sanchez, *Chem. Mater.* **2008**, *20*, 1049 – 1056.
[23] a) S. H. Lee, H. W. Kim, J. O. Hwang, W. J. Lee, J. Kwon, C. W. Bielawski, R. S. Ruoff, S. O. Kim, *Angew. Chem.* **2010**, *122*, 10282 – 10286; *Angew. Chem. Int. Ed.* **2010**, *49*, 10084 – 10088; b) S. Yin, Y. Goldovsky, M. Herzberg, L. Liu, H. Sun, Y. Zhang, F. Meng, X. Cao, D. D. Sun, H. Chen, A. Kushmaro, X. Chen, *Adv. Funct. Mater.* **2013**, *23*, 2972—2978 DOI: 10.1002/adfm.201203491; c) N. Wakamatsu, H. Takamori, T. Fujigaya, N. Nakashima, *Adv. Funct. Mater.* **2009**, *19*, 311 – 316; d) H. Takamori, T. Fujigaya, Y. Yamaguchi, N. Nakashima, *Adv. Mater.* **2007**, *19*, 2535 – 2539.
[24] a) Y. Yu, Y. G. Ma, *Soft Matter* **2011**, *7*, 884 – 886; b) M. Zhang, S. Sun, X. Yu, X. Cao, Y. Zou, T. Yi, *Chem. Commun.* **2010**, *46*, 3553 – 3555; c) S. S. Babu, S. Mahesh, K. K. Kartha, A. Ajayaghosh, *Chem. Asian J.* **2009**, *4*, 824 – 829; d) J. Z. Chen, X. Z. Yan, Q. L. Zhao, L. Li, F. H. Huang, *Polym. Chem.* **2012**, *3*, 458 – 462.
[25] a) A. S. de Leon, A. del Campo, M. Fernandez-Garcia, J. Rodriguez-Hernandez, A. Munoz-Bonilla, *Langmuir* **2012**, *28*, 9778 – 9787; b) A. S. de Leon, J. Rodriguez-Hernandez, A. L. Cortajarena, *Biomaterials* **2013**, *34*, 1453 – 1460; c) F. Galeotti, V. Calabrese, M. Cavazzini, S. Quici, C. Poleunis, S. Yunus, A. Bolognesi, *Chem. Mater.* **2010**, *22*, 2764 – 2769; d) B. B. Ke, L. S. Wan, Z. K. Xu, *Langmuir* **2010**, *26*, 8946 – 8952.
[26] A. Böker, Y. Lin, K. Chiapperini, R. Horowitz, M. Thompson, V. Carreon, T. Xu, C. Abetz, H. Skaff, A. D. Dinsmore, T. Emrick, T. P. Russell, *Nat. Mater.* **2004**, *3*, 302 – 306.
[27] a) P. S. Brown, E. L. Talbot, T. J. Wood, C. D. Bain, J. P. S. Badyal, *Langmuir* **2012**, *28*, 13712 – 13719; b) M. Hernández-Guerrero, E. Min, C. Barner-Kowollik, A. H. E. Müller, M. H. Stenzel, *J. Mater. Chem.* **2008**, *18*, 4718 – 4730; c) E. H. Min, S. R. S. Ting, L. Billon, M. H. Stenzel, *J. Polym. Sci. Part A* **2010**, *48*, 3440 – 3455.
[28] W. Z. Xu, X. Y. Zhang, J. F. Kadla, *Biomacromolecules* **2012**, *13*, 350 – 357.
[29] a) A. Bolognesi, F. Galeotti, J. Moreau, U. Giovanella, W. Porzio, G. Scavia, F. Bertini, *J. Mater. Chem.* **2010**, *20*, 1483 – 1488; b) B. Erdogan, L. Song, J. N. Wilson, J. O. Park, M. Srinivasarao, U. H. F. Bunz, *J. Am. Chem. Soc.* **2004**, *126*, 3678 – 3679.
[30] a) H. Yabu, M. Kojima, M. Tsubouchi, S.-y. Onoue, M. Sugitani, M. Shimomura, *Colloids Surf. A* **2006**, *284 – 285*, 254 – 256; b) L. Li, C. Chen, A. Zhang, X. Liu, K. Cui, J. Huang, Z. Ma, Z. Han, *J. Colloid Interface Sci.* **2009**, *331*, 446 – 452; c) L. Li, C. Chen, J. Li, A. Zhang, X. Liu, B. Xu, S. Gao, G. Jin, Z. Ma, *J. Mater. Chem.* **2009**, *19*, 2789 – 2796; d) Y. Nakamichi, Y. Hirai, H. Yabu, M. Shimomura, *J. Mater. Chem.* **2011**, *21*, 3884 – 3889; e) O. Karthaus, Y. Hashimoto, K. Kon, Y. Tsuriga, *Macromol. Rapid Commun.* **2007**, *28*, 962 – 965; f) L. Wang, S. H. Maruf, D. Maniglio, Y. F. Ding, *Polymer* **2012**, *53*, 3749 – 3755.
[31] a) T. Kabuto, Y. Hashimoto, O. Karthaus, *Adv. Funct. Mater.* **2007**, *17*, 3569 – 3573; b) K. H. Wong, M. H. Stenzel, S. Duvall, F. o. Ladouceur, *Chem. Mater.* **2010**, *22*, 1878 – 1891; c) L. Li, Y. Zhong, J. Gong, J. Li, J. Huang, Z. Ma, *J. Colloid Interface Sci.* **2011**, *354*, 758 – 764.

[32] B. G. Rånby, J. F. Rabek, *Photodegradation, photo-oxidation, and photostabilization of polymers: principles and applications*, Wiley, New York, **1975**.
[33] a) H. Ma, J. Cui, J. Chen, J. Hao, *Chem. Eur. J.* **2011**, *17*, 655 – 660; b) X. L. Jiang, X. F. Zhou, Y. Zhang, T. Z. Zhang, Z. R. Guo, N. Gu, *Langmuir* **2010**, *26*, 2477 – 2483; c) V. Vohra, A. Bolognesi, G. Calzaferri, C. Botta, *Langmuir* **2009**, *25*, 12019 – 12023; d) W. Sun, Z. Shao, J. Ji, *Polymer* **2010**, *51*, 4169 – 4175; e) C. Deleuze, C. Derail, M. H. Delville, L. Billon, *Soft Matter* **2012**, *8*, 8559 – 8562.
[34] R. Aveyard, B. P. Binks, J. H. Clint, *Adv. Colloid Interface Sci.* **2003**, *100 – 102*, 503 – 546.
[35] a) M. H. Nurmawati, R. Renu, P. K. Ajikumar, S. Sindhu, F. C. Cheong, C. H. Sow, S. Valiyaveettil, *Adv. Funct. Mater.* **2006**, *16*, 2340 – 2345; b) J. Zou, H. Chen, A. Chunder, Y. Yu, Q. Huo, L. Zhai, *Adv. Mater.* **2008**, *20*, 3337 – 3341.
[36] X. Xu, L. P. Heng, X. J. Zhao, J. Ma, L. Lin, L. Jiang, *J. Mater. Chem.* **2012**, *22*, 10883 – 10888.
[37] H. Sun, H. Li, L. Wu, *Polymer* **2009**, *50*, 2113 – 2122.
[38] a) K. H. Wong, T. P. Davis, C. Barner-Kowollik, M. H. Stenzel, *Aust. J. Chem.* **2006**, *59*, 539 – 543; b) J. Wang, C.-F. Wang, H.-X. Shen, S. Chen, *Chem. Commun.* **2010**, *46*, 7376 – 7378; c) H. Tsai, Z. Xu, R. K. Pai, L. Wang, A. M. Dattelbaum, A. P. Shreve, H.-L. Wang, M. Cotlet, *Chem. Mater.* **2011**, *23*, 759 – 761; d) J. Wang, H. X. Shen, C. F. Wang, S. Chen, *J. Mater. Chem.* **2012**, *22*, 4089 – 4096; e) L. A. Connal, G. V. Franks, G. G. Qiao, *Langmuir* **2010**, *26*, 10397 – 10400; f) S. H. Lee, J. S. Park, B. K. Lim, C. B. Mo, W. J. Lee, J. M. Lee, S. H. Hong, S. O. Kim, *Soft Matter* **2009**, *5*, 2343 – 2346.
[39] X. Li, L. Zhang, Y. Wang, X. Yang, N. Zhao, X. Zhang, J. Xu, *J. Am. Chem. Soc.* **2011**, *133*, 3736 – 3739.
[40] a) Y. Hirai, H. Yabu, Y. Matsuo, K. Ijiro, M. Shimomura, *Chem. Commun.* **2010**, *46*, 2298 – 2300; b) B. d. Boer, U. Stalmach, H. Nijland, G. Hadziioannou, *Adv. Mater.* **2000**, *12*, 1581 – 1583.
[41] a) D. Ishii, H. Yabu, M. Shimomura, *Colloids Surf. A* **2008**, *313 – 314*, 590 – 594; b) Y. Hirai, H. Yabu, M. Shimomura, *Colloids Surf. A* **2008**, *313 – 314*, 312 – 315; c) H. Yabu, Y. Hirai, M. Shimomura, *Langmuir* **2006**, *22*, 9760 – 9764.
[42] B. B. Ke, L. S. Wan, P. C. Chen, L. Y. Zhang, Z. K. Xu, *Langmuir* **2010**, *26*, 15982 – 15988.
[43] M. Tanaka, K. Yoshizawa, A. Tsuruma, H. Sunami, S. Yamamoto, M. Shimomura, *Colloids Surf. A* **2008**, *313 – 314*, 515 – 519.
[44] a) H. Zhao, Y. Shen, S. Zhang, H. Zhang, *Langmuir* **2009**, *25*, 11032 – 11037; b) K. Kon, C. N. Brauer, K. Hidaka, H.-G. Löhmannsröben, O. Karthaus, *Langmuir* **2010**, *26*, 12173 – 12176.
[45] L. Li, Y. Zhong, C. Ma, J. Li, C. Chen, A. Zhang, D. Tang, S. Xie, Z. Ma, *Chem. Mater.* **2009**, *21*, 4977 – 4983.
[46] a) C. Ma, Y. Zhong, J. Li, C. Chen, J. Gong, S. Xie, L. Li, Z. Ma, *Chem. Mater.* **2010**, *22*, 2367 – 2374; b) J. Gong, L. Sun, Y. Zhong, C. Ma, L. Li, S. Xie, V. Svrcek, *Nanoscale* **2012**, *4*, 278 – 283.
[47] a) B. C. Englert, S. Scholz, P. J. Leech, M. Srinivasarao, U. H. F. Bunz, *Chem. Eur. J.* **2005**, *11*, 995 – 1000; b) H. Ejima, T. Iwata, N. Yoshie, *Macromolecules* **2008**, *41*, 9846 – 9848; c) L. Li, J. Li, Y. Zhong, C. Chen, Y. Ben, J. Gong, Z. Ma, *J. Mater. Chem.* **2010**, *20*, 5446 – 5453.
[48] F. Galeotti, W. Mróz, A. Bolognesi, *Soft Matter* **2011**, *7*, 3832 – 3836.
[49] a) F. Galeotti, A. Andicsova, S. Yunus, C. Botta, *Soft Matter* **2012**, *8*, 4815 – 4821; b) Y. Q. Han, Q. Zhang, F. L. Han, C. X. Li, J. F. Sun, Y. Lu, *Polymer* **2012**, *53*, 2599 – 2603.
[50] a) T. Nishikawa, M. Nonomura, K. Arai, J. Hayashi, T. Sawadaishi, Y. Nishiura, M. Hara, M. Shimomura, *Langmuir* **2003**, *19*, 6193 – 6201; b) X. H. Wu, S. F. Wang, *ACS Appl. Mater. Interfaces* **2012**, *4*, 4966 – 4975.
[51] a) Y. Hirai, H. Yabu, Y. Matsuo, K. Ijiro, M. Shimomura, *J. Mater. Chem.* **2010**, *20*, 10804 – 10808; b) L. Li, Y. Zhong, J. Li, J. Gong, Y. Ben, J. Xu, X. Chen, Z. Ma, *J. Colloid Interface Sci.* **2010**, *342*, 192 – 197; c) M. Haupt, S. Miller, R. Sauer, K. Thonke, A. Mourran, M. Moeller, *J. Appl. Phys.* **2004**, *96*, 3065 – 3069; d) Y. Hirai, H. Yabu, Y. Matsuo, K. Ijiro, M. Shimomura, *Macromol. Symp.* **2010**, *295*, 77 – 80.
[52] a) M. Tanaka, M. Takebayashi, M. Shimomura, *Macromol. Symp.* **2009**, *279*, 175 – 182; b) T. Ponnusamy, L. B. Lawson, L. C. Freytag, D. A. Blake, R. S. Ayyala, V. T. John, *Biomatter* **2012**, *2*, 77 – 86; c) Y. Fukuhira, E. Kitazono, T. Hayashi, H. Kaneko, M. Tanaka, M. Shimomura, Y. Sumi, *Biomaterials* **2006**, *27*, 1797 – 1802; d) H. Sunami, E. Ito, M. Tanaka, S. Yamamoto, M. Shimomura, *Colloids Surf. A* **2006**, *284 – 285*, 548 – 551; e) H. Sun, W. Li, L. Wu, *Langmuir* **2009**, *25*, 10466 – 10472; f) X. Li, Y. Wang, L. Zhang, S. Tan, X. Yu, N. Zhao, G. Chen, J. Xu, *J. Colloid Interface Sci.* **2010**, *350*, 253 – 259.
[53] a) Y. Zhu, R. Sheng, T. Luo, H. Li, J. Sun, S. Chen, W. Sun, A. Cao, *ACS Appl. Mater. Interfaces* **2011**, *3*, 2487 – 2495; b) T. Nishikawa, J. Nishida, R. Ookura, S.-I. Nishimura, S. Wada, T. Karino, M. Shimomura, *Mater. Sci. Eng. C* **1999**, *8 – 9*, 495 – 500.
[54] D. Beattie, K. H. Wong, C. Williams, L. A. Poole-Warren, T. P. Davis, C. Barner-Kowollik, M. H. Stenzel, *Biomacromolecules* **2006**, *7*, 1072 – 1082.
[55] T. Nishikawa, J. Nishida, R. Ookura, S.-I. Nishimura, S. Wada, T. Karino, M. Shimomura, *Mater. Sci. Eng. C* **1999**, *10*, 141 – 146.
[56] S. Duan, X. P. Yang, J. F. Mao, B. Qi, Q. Cai, H. Shen, F. Yang, X. L. Deng, S. G. Wang, *J. Biomed. Mater. Res. Part A* **2013**, *101A*, 307 – 317.
[57] X. Wang, C. A. Ohlin, Q. Lu, J. Hu, *J. Biomed. Mater. Res. Part A* **2006**, *78A*, 746 – 754.
[58] a) F. Galeotti, I. Chiusa, L. Morello, S. Gianì, D. Breviario, S. Hatz, F. Damin, M. Chiari, A. Bolognesi, *Eur. Polym. J.* **2009**, *45*, 3027 – 3034; b) S. R. S. Ting, E. H. Min, P. Escalé, M. Save, L. Billon, M. H. Stenzel, *Macromolecules* **2009**, *42*, 9422 – 9434; c) Y. Zhang, C. Wang, *Adv. Mater.* **2007**, *19*, 913 – 916; d) E. Min, K. H. Wong, M. H. Stenzel, *Adv. Mater.* **2008**, *20*, 3550 – 3556; e) Y. Y. Ma, J. Liang, H. Sun, L. X. Wu, Y. Q. Dang, Y. Q. Wu, *Chem. Eur. J.* **2012**, *18*, 526 – 531.
[59] P. C. Chen, L. S. Wan, B. B. Ke, Z. K. Xu, *Langmuir* **2011**, *27*, 12597 – 12605.
[60] L. S. Wan, Q. L. Li, P. C. Chen, Z. K. Xu, *Chem. Commun.* **2012**, *48*, 4417 – 4419.
[61] H. Yabu, M. Shimomura, *Langmuir* **2005**, *21*, 1709 – 1711.
[62] F. Galeotti, W. Mroz, G. Scavia, C. Botta, *Org. Electron.* **2013**, *14*, 212 – 218.
[63] K. Chari, C. W. Lander, R. J. Sudol, *Appl. Phys. Lett.* **2008**, *92*, 111916.
[64] A. Bolognesi, C. Botta, S. Yunus, *Thin Solid Films* **2005**, *492*, 307 – 312.
[65] M. Pintani, J. Huang, M. C. Ramon, D. D. C. Bradley, *J. Phys. Condens. Matter* **2007**, *19*, 016203.
[66] M. S. Park, J. K. Kim, *Langmuir* **2005**, *21*, 11404 – 11408.
[67] L. Heng, J. Zhai, Y. Zhao, J. Xu, X. Sheng, L. Jiang, *ChemPhysChem* **2006**, *7*, 2520 – 2525.
[68] H. L. Cong, J. L. Wang, B. Yu, J. G. Tang, *Soft Matter* **2012**, *8*, 8835 – 8839.
[69] Y. Xu, B. Zhu, Y. Xu, *Polymer* **2005**, *46*, 713 – 717.
[70] H. Ma, Y. Tian, X. Wang, *Polymer* **2011**, *52*, 489 – 496.
[71] S. Washizu, H. Yamazaki, J. Yamanouchi, H. Naruse (FUJIFILM Corporation), EP20060010988, **2012**.